Published in final edited form as:
Int J Radiat Oncol Biol Phys. 2011 May 1; 80(1): 265–272. doi:10.1016/j.ijrobp.2010.05.023.

Effect of Breathing Motion on Radiotherapy Dose Accumulation in the Abdomen Using Deformable Registration

Michael Velec, B.Sc.[1], **Joanne L. Moseley, B.Math.**[1], **Cynthia L. Eccles, B.Sc.**[1,2], **Tim Craig, Ph.D.**[1,2], **Michael B. Sharpe, Ph.D.**[1,2], **Laura A. Dawson, M.D.**[1,2], and **Kristy K. Brock, Ph.D.**[1,2,3]

[1]Radiation Medicine Program, Princess Margaret Hospital, University Health Network, Toronto, Canada

[2]Department of Radiation Oncology, University of Toronto, Toronto, Canada

[3]Department of Medical Biophysics, University of Toronto, Toronto, Canada

Abstract

Purpose—To investigate the effect of breathing motion and dose accumulation on the planned radiotherapy dose to liver tumors and normal tissues using deformable image registration.

Method and Materials—Twenty one free-breathing stereotactic liver cancer radiotherapy patients, planned on static exhale CT for 27 – 60 Gy in 6 fractions, were included. A biomechanical model-based deformable image registration algorithm, retrospectively deformed each exhale CT to inhale CT. This deformation map was combined with exhale and inhale dose grids from the treatment planning system to accumulate dose over the breathing cycle. Accumulation was also investigated using a simple rigid liver-to-liver registration. Changes to tumor and normal tissue dose were quantified.

Results—Relative to static plans, mean dose change (range) after deformable dose accumulation (as % of prescription dose) was −1 (−14, 8) to minimum tumor, −4 (−15, 0) to max bowel, −4 (−25, 1) to max duodenum, 2 (−1, 9) to max esophagus, −2 (−13, 4) to max stomach, 0 (−3, 4) to mean liver, and −1 (−5, 1) and −2 (−7, 1) to mean left and right kidneys. Compared to deformable registration, rigid modeling had changes up to 8% to minimum tumor and 7% to maximum normal tissues.

Conclusion—Deformable registration and dose accumulation revealed potentially significant dose changes to either a tumor or normal tissue in the majority of cases due to breathing motion. These changes may not be accurately accounted for with rigid motion.

Corresponding Author Info: Michael Velec, B.Sc., M.R.T.(T.). Radiation Medicine Program, Princess Margaret Hospital, University Health Network, 610 University Ave., Toronto, Ontario, Canada, M5G 2M9. Tel (416) 946-4501; Fax (416) 946-6566; michael.velec@rmp.uhn.on.ca.

Presented in part at the 48th Annual Meeting of the American Society of Therapeutic Radiology and Oncology (ASTRO), Philadelphia, PA, November 5–9, 2006.

Keywords

Deformable image registration; respiratory motion; 4D dose calculations; stereotactic body radiotherapy; liver cancer

INTRODUCTION

Radiotherapy for inoperable primary and metastatic liver tumors has become feasible with technological advances in treatment planning and delivery. Stereotactic body radiotherapy (SBRT) has recently been used to deliver highly conformal treatment plans aimed at sparing normal tissue dose, particularly the liver, and allowing dose escalation (1–4).

Liver radiotherapy remains challenging because of respiratory motion (5). At the Princess Margaret Hospital (PMH), the preferred treatment for liver SBRT patients is in controlled exhale breath hold using an active breathing control (ABC) device (6). This technique has good inter and intrafraction reproducibility with online image guidance (6,7). While the impact of respiration on dose with this approach is negligible, many patients are unsuitable for ABC and are treated during free breathing. Therefore, breathing motion should be considered during treatment planning.

Deformable image registration (DIR) algorithms that solve the independent voxel transformations between two images, are a prerequisite to accurate dose accumulation. The effect of breathing on dose has been investigated with DIR of respiration correlated (4D) CT primarily for lung radiotherapy (8–16). Dose reductions to targets (8,14) and increases to normal tissues (13) are sometimes possible. Breathing dose in liver radiotherapy has been studied less in comparison. Challenges with liver radiotherapy not commonly seen with the lung include target volumes directly overlapping adjacent critical structures, and the inability to clearly visualize the tumor on 4D CT due to the lack of contrast. At PMH, liver planning includes individualized planning target volumes and prescription doses. Previous accumulation efforts on liver radiotherapy often used dose(5) or fluence(17) convolution with probability distribution functions that model respiration motion, though these effectively model breathing with rigid-body motion.

Kaus *et al*. (18) investigated DIR of exhale and inhale abdominal MR images using corresponding organ surface-meshes and elastic-body or thin-plate splines, achieving accuracy near the image resolution. Image intensity-driven algorithms, such as B-splines with normalized mutual information (19,20), have also been investigated. Brock *et al*.(21) demonstrated multi-organ registration is accurate using a biomechanical model-based algorithm. Brock *et al*. (22) accumulated dose for four patients' livers by deforming exhale to inhale CT. Compared to static plans, changes in the allowable prescribed tumor dose from −4.1 to 1.7 Gy were seen, suggesting the dosimetric effects of breathing may be clinically significant. This study involved simulated tumors and plans however, omitting the complexities seen in plans where clinicians must adhere to strict trial protocols. Further investigation is warranted to study organs at risk, which often limit the safe doses that may be delivered despite highly conformal planning (23).

This study investigates accumulated breathing dose to targets and normal tissues for liver radiotherapy planning using biomechanical model-based deformable registration. Breathing dose was accumulated with the unaltered clinical plans, initially optimized on exhale CT, to provide a realistic account of the information that can be derived with DIR under current planning techniques. A secondary aim was to compare dose accumulation using simple rigid-body motion to DIR. This is essential in understanding respiration, the largest

geometric uncertainty in radiotherapy, on planning where critical decisions must be made regarding tumor dose, to improve disease control, and normal tissue dose, to avoid toxicity.

METHODS AND MATERIALS

Patient details and imaging

This study included 21 liver cancer patients previously treated on a Research Ethics Board (University Health Network) approved protocol of Phase I/II dose-escalation, hypofractionated liver SBRT. Patients had primary liver cancer (n=8) or liver metastases (n=13). The number of tumors ranged from 1 (n=15) to 6 (n=1). Subjects in this analysis were unsuitable for ABC treatment due to small breathing amplitude (<0.5 cm), inconsistent breath-hold position, diaphragm drifts, and compliance issues or tolerance of the device. All were treated during normal free breathing (n=15) or free breathing plus abdominal compression plate (n=6).

Patients were supine with arms above head and immobilized using an evacuated cushion (n=16), chest board (n=1) or an SBRT body frame (n=4). Planning was done on helical CT acquired during voluntary normal exhale breath-hold (n=15), or on the end exhale breathing phase from 4D CT (n=6). Inhale CT was acquired during 4D CT, or immediately following the exhale scan using a voluntary normal inhale breath hold, to assess breathing motion. 4D CT images were reconstructed by binning images using phase-based sorting of an infrared tracked reflective external marker. CT imaging had an average resolution of 0.1×0.1×0.3 cm^3. In addition to 4D CT, fluoroscopic measurement of diaphragm motion (amplitude range: 0.5 – 3.0 cm, mean: 1.3 cm) and cine-MRI of the tumor were done when possible to aid in determination of individualized margins as direct 3D tumor motion is poorly visualized on 4D CT, despite the use of contrast agents.

Treatment planning

Planning and delineation was done on a static exhale CT data set using a commercial treatment planning system (Pinnacle^3 v6.2 – 8.1, Philips Medical Systems, Madison WI). Volumes were generated as per the clinical protocol as follows. Gross tumor volumes (GTV) were isotropically expanded 0.8 cm within the liver to create clinical target volumes (CTV). Individualized, asymmetric internal margins (IM) were generally created by estimating 90% of the maximum motion from the baseline exhale position seen on the 2D imaging studies. This avoid unnecessarily large IM that might be exaggerated by short lived, large maximum inhales, as the end inhale position is less stable than exhale(24). These maximum motions, easily captured on 2D imaging, are not as discernable on 4D CT due to multiple breathing patterns combined to form each dataset, which naturally will reduce the maximum motion. A 0.3 cm setup margin (SM) for daily positioning error was added to each patient specific IM to create planning target volumes (PTV). Although setup uncertainties are not modeled in this study, this expansion was included to evaluate normal tissues moving in and out of the realistically irradiated volume during respiration. PTV (IM + SM) ranged from 0.5 – 1.0 cm left and anterior, 0.5 – 0.7 cm right, 0.5 – 0.6 cm posterior and superior, and 0.8 – 2.5 cm inferior. A PTV was first applied around the GTV creating a PTV_{GTV}. The same PTV margin was also applied around the CTV (GTV + 0.8 cm in liver) creating a PTV_{CTV}.

Coplanar or non-coplanar beam arrangements were placed to minimize path length through the liver. The number of beams, including forward planned segments, ranged from 5 – 21 (median: 8). Planning objectives used (Table 1) varied as the clinical protocols evolved. Respecting normal tissue constraints was mandatory. Maintaining PTV_{GTV} coverage was

the primary goal, while coverage of the larger PTV_{CTV} was a secondary aim with lower dose criteria.

Dose was individually prescribed by determining the risk of radiation-induced liver disease from the Lyman NTCP model (25), based in part by diagnosis (primary or metastases), the assigned NTCP level per study protocol (5 – 20%), and the liver effective volume (V_{eff}). V_{eff} is the uninvolved liver volume uniformly irradiated to the prescription, and estimated to have an equivalent complication risk as non-uniform irradiation(26). The mean dose was 39 Gy (range: 27 – 60 Gy) in 6 fractions over two weeks, limited mostly by liver and luminal gastrointestinal dose constraints.

Deformable image registration

A multi-organ biomechanical model-based DIR algorithm (Morfeus) developed in-house, deformed 4D CT images allowing tissue tracking across the breathing cycle. This algorithm, previously described in detail (21,27), is summarized here.

Primary contours from the exhale CT plan are converted into 3D surface meshes and filled with tetrahedral elements creating a base model of the patient. Contours minimally included the liver, GTV(s), external body, spleen and organs at risk. The deformation and motion of the model is driven by guided surface projections of the primary surface meshes into secondary surfaces created from additional inhale CT contours of the liver, external body and spleen. All tetrahedral elements, including organs and GTV(s) without additional inhale contours, are implicitly deformed according to biomechanical tissue properties (Table 2) using finite element analysis. The result is a displacement map from exhale to inhale. The accuracy of Morfeus for all deformed tissues is less than 0.2 cm(21).

Dose calculations

Dose was calculated in the planning system on exhale CT using a convolution-superposition algorithm and heterogeneity corrections, with a matrix resolution of $0.25\times0.25\times0.25$ cm^3. Plans were also calculated on the inhale CT providing two dose extremes occurring during breathing. Dose accumulation using extracted matrices was performed in the DIR research environment. From DIR, the locations and size of every element in the model during breathing are known. Four intermediate positions and volumes between exhale and inhale are linearly interpolated for each element representing intermediate phases. The element centroid at every step is interpolated onto each matrix, where the dose contribution is weighted to the element's position in the breathing cycle. For example, the exhale matrix will contribute greater dose to an element closer to exhale. This simplification avoids intermediate phases' matrices, as the majority of patients lacked 4D CT. Steps are additionally weighted according to time spent in that phase (Table 3), based on previously studied patients (28). Element dose was summed across the breathing cycle as follows (22):

$$\mathrm{D}(x,y,z)=\sum_{\varphi=0}^{1}\left[\left[D_{\varphi}^{E}\left(\mathrm{x}+\varphi\Delta_{\mathrm{x}},\mathrm{y}+\varphi\Delta_{\mathrm{y}},\mathrm{z}+\varphi\Delta_{\mathrm{z}}\right)[1-\varphi]\right]+\left[D_{\varphi}^{\mathrm{I}}\left(\mathrm{x}+\varphi\Delta_{\mathrm{x}},\mathrm{y}+\varphi\Delta_{\mathrm{y}},\mathrm{z}+\varphi\Delta_{\mathrm{z}}\right)\varphi\right]\right]\left(\mathrm{T}_{\varphi}\right)$$

where $D(x, y, z)$ is the element dose at coordinates x, y, z, D_{ϕ}^{E} and D_{ϕ}^{I} are the relative contributions from the exhale and inhale dose matrices respectively, φ is the breathing phase (range is 0 [exhale] to 1 [inhale] in increments of 0.2), $\varphi\Delta_x$, $\varphi\Delta_y$, $\varphi\Delta_z$ is the translation of the element from the deformation map, T_{φ} is the time weighting factor for phase φ.

Dosimetric analysis

Three scenarios were compared:

1) Static distributions calculate dose solely on exhale CT, replicating clinical practice without motion. Elements in exhale are interpolated onto the exhale dose grid within the DIR environment, to facilitate their comparison to the following.

2) Distributions that accumulate breathing dose using the rigid liver centre-of-mass (COM) breathing motion applied to the entire model. Liver COM was chosen over the GTV as direct tumor visualization is poor and often impossible on 4D CT, impossible with fluoroscopy, and the use of cine-MRI (for direct visualization of the tumor) is not standard in most clinics. Meaning, clinicians would likely not have the true 3D GTV COM information without DIR.

3) Breathing dose accumulation incorporating DIR uses the full multi-organ deformation map.

Changes greater than 1 Gy were considered potentially significant, though are here as a percent change (normalized to the prescription dose). Differences in liver NTCP and V_{eff} were also quantified. To assess the potential clinical impact of breathing dose accumulation on planning, clinical plans were reviewed to determine if target coverage was compromised due to normal tissues. Normal tissues within 2 Gy of the limit (Table 1) were identified as having potentially influenced planning.

RESULTS

Breathing motion

Breathing COM motion from DIR is summarized in Table 4. Rigid modeling used liver COM motion, while static plans did not consider motion.

After DIR, nine patients (43%) had GTV COM motion that exceeded the initial PTV_{GTV}. These excursions occurred in the left (n=4, range: 0.1 – 1.0 cm), anterior (n=6, range: 0.2 – 1.0 cm) and inferior (n=6, range: 0.1 – 0.3 cm) directions. Liver COM motion similarly predicted these GTV excursions in all but one case, where rigid liver COM motion underestimated the GTV motion from DIR by 0.3 cm, due to liver deformation.

Differences of at least 0.3 cm between liver and GTV COM motion after DIR were observed in eleven (52%) cases. Average absolute differences (maximum) were 0.1 (0.6), 0.2 (0.7), and 0.2 (1.0) cm in the left-right, anterior-posterior, and superior-inferior directions respectively. DIR revealed differences in intrahepatic GTV motion for multifocal cases (Fig. 1). Six of seven patients with multiple tumors had GTV COM differences greater than 0.3 cm in at least one direction, up to a maximum of 1.0 cm in the left-right and anterior-posterior directions, and 0.8 cm superior-inferiorly. These would not have been accounted for with rigid liver motion alone.

Effects of dose accumulation

Dosimetric changes with rigid and deformable breathing dose accumulation are shown in Table 5. Changes of at least 1 Gy to the minimum GTV dose, or maximum or mean normal tissue dose were observed in all but one patient (95%) when comparing deformable dose accumulation to static plans. A breathing dose distribution using DIR is shown in Fig 2. Rigid accumulation caused discrepancies greater than 1 Gy in ten patients (48%) compared DIR, resulting in changes up to 8% in tumors and 7% in normal tissues.

Patients with over 1.0 cm of liver motion had higher average absolute changes with DIR compared to static, than small breathers. This was significant for the minimum GTV dose (increase of 2.7% with DIR, p=0.004), mean dose to the liver (2.8%, p=0.003), right (13.8%, p <0.000) and left (7.5%, p=0.02) kidneys and maximum duodenum dose (13.4%, p=0.004). Dose to remaining organs for large breathers was also generally higher (p>0.05).

Potential changes to planning constraints

In order to respect normal tissue constraints in ten patients, GTV (n=2) or PTV_{GTV} (n=8) dosimetric criteria (Table 1) were compromised on the initial clinical plans based on static exhale CT. After deformable dose accumulation, the minimum dose to 0.5 cm^3 in any one GTV changed in five patients by −11.9% – 3.7%. For two of these cases, rigid accumulation had differences compared to DIR of −5.0% and 4.2%. Figure 3 demonstrates changes to tumors and normal tissues among the three dose distributions.

Bowels were limiting organs in 8 patients (38%). The maximum dose to 0.5 cm^3 decreased in four cases with DIR by −13.1 – −6.2%. For one patient, DIR predicted a difference of −0.8% whereas rigid accumulation incorrectly predicted −4.0%. Stomach and esophagus were limiting organs for seven (33%) and five (24%) patients respectively. With DIR, the maximum dose to 0.5 cm^3 changed in three stomach cases by −9.3 – 3.3%, and increased by 8.9% and 4.0% for two esophagus cases. A maximum difference of −2.4% was observed for one stomach case between rigid and deformable accumulation. Duodenum was a limiting organ for three patients (14%). DIR reduced the maximum dose to 0.5 cm^3 in two cases by −6.9% and −7.9%. Rigid accumulation had a discrepancy of 2.9% compared to DIR for one patient. Right or left kidney dose was a limiting organ for seven patients (33%). DIR reduced the mean dose in three cases, corresponding to changes of −6.6 – −2.7 %. A maximum difference of 2.5% between rigid accumulation and DIR was seen for one patient.

Changes in liver V_{eff} and NTCP are shown in Table 6. Seven patients (29%) had changes in liver NTCP greater than 5% when breathing motion was modeled with either deformable or rigid registration.

Overall, ten patients failed to meet constraints to either the GTV or PTV_{GTV} on the clinical exhale plans without exceeding normal tissue doses. With deformable dose accumulation, five patients had further reductions to minimum tumor dose and two of these also had increases to esophagus or stomach that would have exceeded dose constraints.

DISCUSSION

Dose distributions incorporating breathing motion were calculated for 21 SBRT liver patients using deformable registration of exhale and inhale CT. Compared to static dose, DIR resulted in dose changes of at least 5% in 12 of 21 patients (57%), to at least one target volume or normal tissue structure. Rigid-body accumulation compared to DIR caused a dose difference of at least 5% in 2 patients (9.5%). To our knowledge, this is the largest series investigating multi-organ deformable registration on breathing dose accumulation for liver radiotherapy.

Patients were on a hypo-fractionated protocol that prescribed dose based on estimated liver NTCP(25), though normal tissue dose constraints commonly limited the prescription and minimum GTV or PTV_{GTV} dose. Ten patients had known dose compromises to targets which resulted in more significant changes to the minimum GTV dose in five patients after DIR. It is important to emphasize the relative difference in breathing dose accumulation versus static plans however, and not the specific planning technique used. Patients could have been prescribed to a lower isodose, thereby eliminating the compromised target dose

but increasing unwanted hot spots. Accurate knowledge of doses planned in the presence of breathing motion would allow more informed tumor dose-toxicity risk tradeoffs to be made, potentially reducing patient risks or improving dose escalation. Deformable registration for breathing dose accumulation at the time of plan optimization may be beneficial for these cases. All cases where minimum tumor dose decreased with DIR had either initially compromised target coverage or tumor motion that exceeded the original PTV_{GTV}.

DIR provided important geometric information in addition to dose accumulation. In nine cases, tumor motion exceeded the boundaries of the PTV_{GTV} by 0.1 – 1.0 cm, with three being ≥ 0.5 cm. Liver and diaphragm motion, assessed using 4D CT, and tumor motion, assessed using cine-MRI, were compared to rigid liver COM motion for the nine cases to see if the clinical PTV_{GTV} margins were initially underestimated. Three cases revealed that rigid liver COM motion was smaller than the PTV_{GTV} yet the GT motion from DIR exceeded it. This indicates complex deformation-motion not accounted for in margins based on rigid 4D CT liver motion, or motion observed with fluoroscopy. This is possible as liver regions can move and deform more than the whole liver (Figure 1). Four cases had rigid liver COM motion greater than the motion based on the diaphragm, indicating a simple liver rigid registration may better predict motion than the method used clinically. Finally, two cases had rigid liver COM and diaphragm motion larger than the PTV boundaries by 0.6 cm anterior and 0.5 cm left. For three cases with extreme excursions (≥ 0.5 cm), a review of the cine-MRI revealed that even direct visualization of the tumor motion in 2D may not adequately capture the complex deformation-motion revealed with deformable registration of 3D images. The GTV was visualized on 4D CT for one of these cases, and after careful review of all slices and planes the DIR predicted motion was confirmed. Future studies could investigate how well 2D motion studies predict 3D deformation-motion.

Patients could have been re-planned with PTV_{GTV} revised using the DIR predicted GTV motion. However this retrospective study was designed to capture the impact DIR has on current planning techniques. Larger margins may improve GTV dose, at a cost of increased liver NTCP and larger changes to normal tissues due to the larger irradiated volume. Setup uncertainties, not modeled in this study, are assumed to be small as patients are treated with soft-tissue image-guidance and a 0.3 cm tolerance level, much smaller than the breathing motion.

Liver COM motion was used to model rigid-body motion in this study. GTV COM was not used as this would have required the results of DIR of 4D CT. Unlike in the lung, liver tumors are often poorly visualized on 4D CT despite intravenous contrast(29), prohibiting the use of rigid registration to accurately measure GTV COM. Additionally, the effect of choosing COM of the GTV versus the liver, a relatively large organ, as a surrogate for all motion within the abdomen is unknown, as large differences between GTV and liver COM, or between GTV COM for multifocal cases, were sometimes observed.

DIR was used on voluntary breath hold CT, or free breathing 4D CT. Breath hold CT may exaggerate motion if patients' took deep breaths during imaging. To reduce this possibility, patients were instructed to breathe normally. Additionally for this study, superior-inferior liver motion from DIR was compared to the fluoroscopy motion and was generally found to not exceed this (maximum observed increase from DIR was 0.3 cm).

Dose changes were observed with minimal breathing, however, patients with over 1.0 cm of motion had significantly greater changes to most tissues suggesting this subgroup may benefit more from DIR during planning optimization. Factors confounding the magnitude of dose change are the relative distance between organs and targets, and variability in planning techniques or dose gradients, though these are subject to ongoing analysis. Wu *et al.* (20)

accumulated liver SBRT breathing dose using thin plate splines on five patients' 4D CT images and demonstrated intensity-modulated radiotherapy may be more sensitive to breathing motion than conventional plans.

Exhale and inhale 4D CT was used, with a linear interpolation providing intermediary breathing positions. Future work will investigate integrating intermediate 4D CT phases as hysteresis and motion non-linearity have been observed in other studies(30). Patient specific breathing patterns extracted from 4D CT could also be integrated into DIR, though research suggests variations in pattern asymmetry is unlikely to significantly impact dose (5,15). Although geometric validation of DIR algorithms has been done, dosimetric validation of 4D calculations in deforming anatomy is complicated by a lack of precise enough phantoms to establish a control. Work in underway to address this using deformable gel dosimeters.

Breathing dose accumulation at planning is valid if the motion during treatment is consistent. Accumulating dose over the entire treatment course using daily breathing models acquired with 4D cone-beam CT (31) is also possible with DIR. Better accounting of dose to targets and normal tissues in the presence of geometric uncertainty may improve understanding of dose-response outcomes for normal tissue toxicity and tumor control.

CONCLUSIONS

Deformable image registration between exhale and inhale CT, allows tissue tracking and breathing dose accumulation. Potentially significant dose changes were observed in the majority of patients to either a tumor or normal tissue, compared to static plans. Understanding breathing dose accumulation may help identify which liver patients, previously limited in prescribed dose because of normal tissues, may be safely escalated to higher doses with more realistic modeling at planning.

Acknowledgments

This work is supported by the National Cancer Institute of Canada – Terry Fox Foundation, and U.S. National Institutes of Health – 5RO1CA124714-02. Patients were treated on clinical trials supported by the Canadian Cancer Society (Grant 18207) and Elekta Oncology Systems. K. K. Brock is supported by a research chair from Cancer Care Ontario.

CONFLICT OF INTEREST NOTIFICATION Dr. Brock receives grant support from Elekta Oncology Systems, Philips Medical Systems, RaySearch Laboratories, and serves on the IMPAC Physics Advisory Board. Dr. Dawson receives grant support from Bayer and Elekta Oncology Systems.

REFERENCES

1. Lee MT, Kim JJ, Dinniwell R, et al. Phase I study of individualized stereotactic body radiotherapy of liver metastases. J Clin Oncol. 2009; 27:1585–1591. [PubMed: 19255313]
2. Tse RV, Hawkins M, Lockwood G, et al. Phase I study of individualized stereotactic body radiotherapy for hepatocellular carcinoma and intrahepatic cholangiocarcinoma. J Clin Oncol. 2008; 26:657–664. [PubMed: 18172187]
3. Rusthoven KE, Kavanagh BD, Cardenes H, et al. Multi-institutional phase I/II trial of stereotactic body radiation therapy for liver metastases. J Clin Oncol. 2009; 27:1572–1578. [PubMed: 19255321]
4. Katz AW, Carey-Sampson M, Muhs AG, et al. Hypofractionated stereotactic body radiation therapy (SBRT) for limited hepatic metastases. Int J Radiat Oncol Biol Phys. 2007; 67:793–798. [PubMed: 17197128]
5. Lujan AE, Balter JM, Ten Haken RK. A method for incorporating organ motion due to breathing into 3D dose calculations in the liver: sensitivity to variations in motion. Med Phys. 2003; 30:2643–2649. [PubMed: 14596301]

6. Dawson LA, Eccles C, Bissonnette JP, et al. Accuracy of daily image guidance for hypofractionated liver radiotherapy with active breathing control. Int J Radiat Oncol Biol Phys. 2005; 62:1247–1252. [PubMed: 15990028]
7. Eccles C, Brock KK, Bissonnette JP, et al. Reproducibility of liver position using active breathing coordinator for liver cancer radiotherapy. Int J Radiat Oncol Biol Phys. 2006; 64:751–759. [PubMed: 16458774]
8. Starkschall G, Britton K, McAleer MF, et al. Potential dosimetric benefits of four-dimensional radiation treatment planning. Int J Radiat Oncol Biol Phys. 2009; 73:1560–1565. [PubMed: 19231098]
9. Admiraal MA, Schuring D, Hurkmans CW. Dose calculations accounting for breathing motion in stereotactic lung radiotherapy based on 4D-CT and the internal target volume. Radiother Oncol. 2008; 86:55–60. [PubMed: 18082905]
10. Ehler ED, Tome WA. Lung 4D-IMRT treatment planning: an evaluation of three methods applied to four-dimensional data sets. Radiother Oncol. 2008; 88:319–325. [PubMed: 18703249]
11. Flampouri S, Jiang SB, Sharp GC, et al. Estimation of the delivered patient dose in lung IMRT treatment based on deformable registration of 4D-CT data and Monte Carlo simulations. Phys Med Biol. 2006; 51:2763–2779. [PubMed: 16723765]
12. Glide-Hurst CK, Hugo GD, Liang J, et al. A simplified method of four-dimensional dose accumulation using the mean patient density representation. Med Phys. 2008; 35:5269–5277. [PubMed: 19175086]
13. Hugo GD, Campbell J, Zhang T, et al. Cumulative lung dose for several motion management strategies as a function of pretreatment patient parameters. Int J Radiat Oncol Biol Phys. 2009; 74:593–601. [PubMed: 19327911]
14. Kang Y, Zhang X, Chang JY, et al. 4D Proton treatment planning strategy for mobile lung tumors. Int J Radiat Oncol Biol Phys. 2007; 67:906–914. [PubMed: 17293240]
15. Rosu M, Balter JM, Chetty IJ, et al. How extensive of a 4D dataset is needed to estimate cumulative dose distribution plan evaluation metrics in conformal lung therapy? Med Phys. 2007; 34:233–245. [PubMed: 17278509]
16. Rosu M, Chetty IJ, Balter JM, et al. Dose reconstruction in deforming lung anatomy: dose grid size effects and clinical implications. Med Phys. 2005; 32:2487–2495. [PubMed: 16193778]
17. Chetty IJ, Rosu M, Tyagi N, et al. A fluence convolution method to account for respiratory motion in three-dimensional dose calculations of the liver: a Monte Carlo study. Med Phys. 2003; 30:1776–1780. [PubMed: 12906195]
18. Kaus MR, Brock KK, Pekar V, et al. Assessment of a model-based deformable image registration approach for radiation therapy planning. Int J Radiat Oncol Biol Phys. 2007; 68:572–580. [PubMed: 17498570]
19. Rohlfing T, Maurer CR Jr. O'Dell WG, et al. Modeling liver motion and deformation during the respiratory cycle using intensity-based nonrigid registration of gated MR images. Med Phys. 2004; 31:427–432. [PubMed: 15070239]
20. Wu QJ, Thongphiew D, Wang Z, et al. The impact of respiratory motion and treatment technique on stereotactic body radiation therapy for liver cancer. Med Phys. 2008; 35:1440–1451. [PubMed: 18491539]
21. Brock KK, Sharpe MB, Dawson LA, et al. Accuracy of finite element model-based multi-organ deformable image registration. Med Phys. 2005; 32:1647–1659. [PubMed: 16013724]
22. Brock KK, McShan DL, Ten Haken RK, et al. Inclusion of organ deformation in dose calculations. Med Phys. 2003; 30:290–295. [PubMed: 12674227]
23. Eccles CL, Bissonnette JP, Craig T, et al. Treatment planning study to determine potential benefit of intensity-modulated radiotherapy versus conformal radiotherapy for unresectable hepatic malignancies. Int J Radiat Oncol Biol Phys. 2008; 72:582–588. [PubMed: 18793961]
24. Seppenwoolde Y, Shirato H, Kitamura K, et al. Precise and real-time measurement of 3D tumor motion in lung due to breathing and heartbeat, measured during radiotherapy. Int J Radiat Oncol Biol Phys. 2002; 53:822–834. [PubMed: 12095547]
25. Dawson LA, Eccles C, Craig T. Individualized image guided iso-NTCP based liver cancer SBRT. Acta Oncol. 2006; 45:856–864. [PubMed: 16982550]

26. Kutcher GJ, Burman C, Brewster L, et al. Histogram reduction method for calculating complication probabilities for three-dimensional treatment planning evaluations. Int J Radiat Oncol Biol Phys. 1991; 21:137–146. [PubMed: 2032884]

27. Brock KK, Dawson LA, Sharpe MB, et al. Feasibility of a novel deformable image registration technique to facilitate classification, targeting, and monitoring of tumor and normal tissue. Int J Radiat Oncol Biol Phys. 2006; 64:1245–1254. [PubMed: 16442239]

28. Lujan AE, Larsen EW, Balter JM, et al. A method for incorporating organ motion due to breathing into 3D dose calculations. Med Phys. 1999; 26:715–720. [PubMed: 10360531]

29. Wang H, Krishnan S, Wang X, et al. Improving soft-tissue contrast in four-dimensional computed tomography images of liver cancer patients using a deformable image registration method. Int J Radiat Oncol Biol Phys. 2008; 72:201–209. [PubMed: 18722271]

30. Boldea V, Sharp GC, Jiang SB, et al. 4D-CT lung motion estimation with deformable registration: quantification of motion nonlinearity and hysteresis. Med Phys. 2008; 35:1008–1018. [PubMed: 18404936]

31. Sonke JJ, Zijp L, Remeijer P, et al. Respiratory correlated cone beam CT. Med Phys. 2005; 32:1176–1186. [PubMed: 15895601]

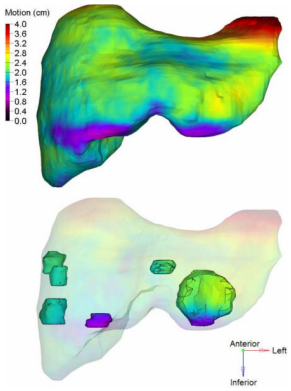

Fig 1.

Example of an exhale liver (top), and intrahepatic GTVs (bottom). The 3D motion map overlaid is found by deforming the exhale to inhale CT. Regions of the liver move 4 cm in this case, due to breathing induced deformation.

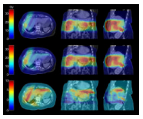

Fig 2.
Dose distribution changes are shown on exhale CT (in Gy). Six GTVs were prescribed 32.4 Gy in 6 fractions. Top: Static dose. Middle: Dose accumulation with DIR. Bottom: Difference between DIR and static plans.

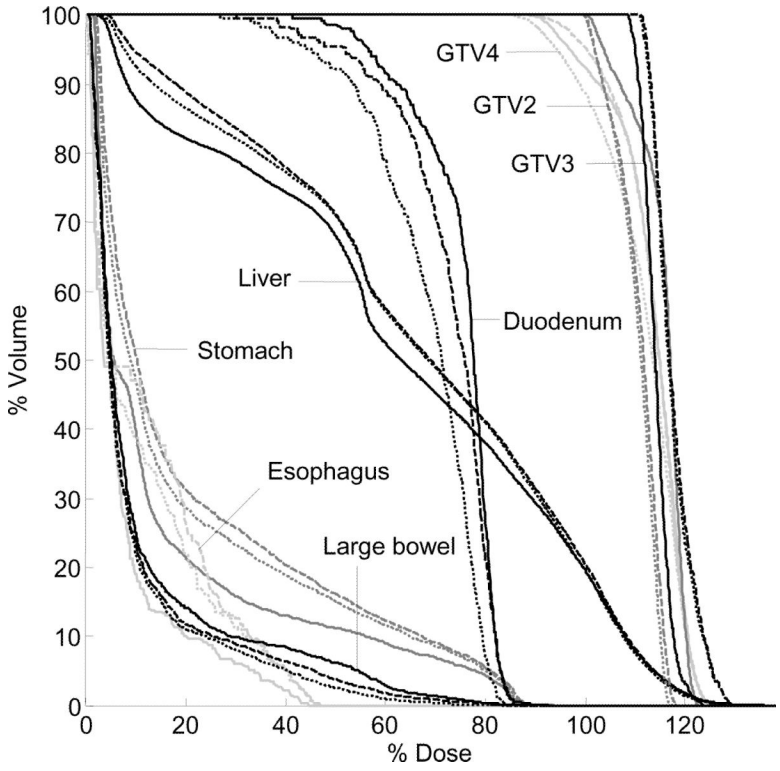

Fig 3.

Example DVH highlighting changes to targets and normal tissues for three calculations: static (solid line) and dose accumulation with either DIR (dashed line) or; rigid liver motion (dotted line).

Table 1

Target and normal tissue planning criteria, for 6 fractions.

Region of interest	Dose criteria	Limit*	Limit if the PTV overlaps non-liver normal tissues
GTV	Min to 0.5 cm^3	95% of prescription	n/a
PTV_{GTV}†	Min (max) to 0.5 cm^3 volume	95% (140%) of prescription	80% of prescription
PTV_{CTV}†	Min to 0.5 cm^3	27.0 Gy	n/a
Large Bowel	Max to 0.5 cm^3	28.2 Gy	30.0 Gy
Small Bowel	Max to 0.5 cm^3	28.2 – 33.6 Gy	30.0 – 36.0 Gy
Stomach	Max to 0.5 cm^3	28.2 – 30.0 Gy	30.0 – 33.6 Gy
Duodenum, esophagus	Max to 0.5 cm^3	28.2 Gy	30.0 Gy
Kidney(s)	Mean to one or combined kidneys	10 Gy	n/a

Abbreviations: GTV = gross tumor volume; CTV = clinical target volume (GTV plus 0.8 cm expansion in liver); PTV = planning target volume (patient specific internal margin for breathing plus 0.3 cm setup margin expansion); PTV_{GTV} = PTV applied around the GTV; PTV_{CTV} = PTV applied around the CTV.

Notes:

* Ranges indicate criteria was modified during the course of the trial

† For each patient the same PTV expansion was applied to each the GTV and CTV though dose criteria was different.

Table 2

Linear elastic material properties used by MORFEUS.

	Poisson's ratio	Young's modulus (kPa)
Liver, esophagus, heart	0.450	7.8
Liver tumor	0.450	78.0
Stomach	0.499	500.0
Bowel, duodenum	0.499	10.0
Spleen	0.499	50.0
Kidneys	0.499	24.0
Other body tissues	0.400	1.5

Table 3

Time weighting factors for each breathing phase[28].

Breathing phase, φ	Relative time weight, Tφ
0 (exhale)	0.48
0.2	0.13
0.4	0.09
0.6	0.08
0.8	0.10
1 (inhale)	0.12

Table 4

Average (range) centre-of-mass motion from deformable registration of exhale to inhale CT (in cm).

Organ	Left-right	Anterior-posterior	Superior-Inferior	3D Vector magnitude
GTV(s) (n=42)	−0.2 (−1.5, 0.4)	0.6 (−0.1, 1.7)	1.0 (0.1, 2.1)	1.3 (0.3, 2.5)
Liver (n=21)	−0.2 (−1.0, 0.3)	0.5 (0.1, 1.3)	1.0 (0.3, 1.8)	1.2 (0.5, 2.1)
Thoracic organs (esophagus, heart) (n= 35)	−0.1 (−0.6, 0.3)	0.3 (0, 0.9)	1.0 (0.3, 2.7)	1.1 (0.3, 2.8)
Abdomimal organs (stomach, bowel duodenum, spleen, right/left kidney) (n= 122)	−0.1 (−0.9, 0.9)	0.5 (−0.2, 2.1)	1.0 (0.1, 5.9)	1.2 (0.1, 6.3)

Abbreviations: GTV=gross tumor volume. Notes: Positive values indicate motion in the left, anterior, or inferior directions.

Table 5

Average change (range) per tissue for different dose distributions (in % change of prescription dose).

Tissue	Criteria	MORFEUS vs. static	Rigid-body vs. static	MORFEUS vs. rigid-body
GTV(s) (n=42)	Δ Min	−0.9 (−14.2, 8.0)	−0.8 (−10.6, 6.6)	0 (−5.1, 8.3)
Liver* (n=21)	Δ Mean	−0.3 (−3.2, 4.0)	−0.4 (−3.3, 3.0)	0.2 (−0.2, 1.0)
Left Kidney (n=21)	Δ Mean	−0.6 (−4.6, 0.8)	−0.6 (−3.6, 1.1)	−0.1 (−2.5, 0.9)
Right Kidney (n=21)	Δ Mean	−1.6 (−6.6, 1.1)	−1.7 (−7.1, 0.9)	0.1 (−0.2, 0.7)
Bowel† (n=21)	Δ Max	−3.5 (−15.0, 0.2)	−4.2 (−13.6, 0.3)	0.7 (−3.9, 7.2)
Duodenum (n=19)	Δ Max	−3.8 (−24.7, 0.8)	−4.0 (−25.2, 0.2)	0.2 (−4.0, 2.0)
Esophagus (n=19)	Δ Max	1.9 (−1.3, 9.1)	1.8 (−1.3, 9.6)	0.1 (−0.5, 1.4)
Stomach (n=19)	Δ Max	−1.6 (−13.4, 4.1)	−1.7 (−13.3, 6.0)	0.2 (−1.9, 2.7)
Heart (n=16)	Δ Max	3.5 (−0.7, 12.8)	3.7 (−0.7, 11.4)	−0.3 (−4.2, 3.3)

Abbreviations: GTV = gross tumor volme

Notes:

* Liver minus GTV.

† Includes large or small bowel. Note: Min and max doses are reported to a single element.

Table 6

Average absolute change (and actual range) in liver V_{eff} and NTCP.

Comparison	Δ V_{eff} (% volume)	Δ % NTCP
MORFEUS vs. static	1.2 (−3.2, 4.0)	3.2 (−15.7, 5.3)
Rigid body vs. static	1.2 (−3.4, 3.0)	3.1 (−15.4, 4.2)
MORFEUS vs. Rigid body	0.2 (−0.2, 1.0)	0.3 (−0.3, 1.8)

Abbreviations: V_{eff} = effective volume; NTCP = normal tissue complication probability.